◻ 93

Dynamic modeling of the birefringence effects induced in semiconductor optical amplifier for all-optical telecommunication systems

Elyamani[1], A. Zatni[2], A. Moumen[3], H. Bousseta[4]
[1,3,4]L. M.T.I Laborator, Department of Physics, Faculty of Science, Ibn Zohr University Agadir, Morocco.
[2]Department of Physics, Faculty of Science Agadir, Morocco

Article Info	ABSTRACT

The semiconductor optical amplifiers (SOA) are all-optical multifunctional devices. The improvement of their performance will, therefore, be of great importance for modern optical telecommunication systems. We propose in this article to develop a dynamic model that enables us to simulate the dynamic behavior of SOA's birefringence effects. The determination of a numerical model is a multidisciplinary activity that needs engineering skills, optimization and physics. This numerical model enables to describe the propagation of a picosecond optical pulse passing through the SOA and takes into account its polarization and the phenomenon of energy coupling between the eigenmodes of SOA (TE mode and TM mode). In this paper, we will, first of all describe the numerical algorithm of our model, and then we will propose to make a dynamic characterization of the effect of the nonlinear polarization rotation in the SOA, which will allow us to study the all-optical logic gates as well as all the other digital components based on the nonlinear effect of birefringence in SOA.

Corresponding Author:

A. Elyamani,
L. M.T.I Laborator, Department of Physics, Faculty of Science,
Ibn Zohr University Agadir,
Nouveau complexe universitaire ‹Agadir 80000, Maroko.
Email: abdenbi.elyamani@gmail.com

1. INTRODUCTION (10 PT)

Semiconductor Optical Amplifiers (SOAs) are expected to become key elements in optoelectronic integrated systems and fiber transmission systems [1-3]. There has been considerable progress in exploitation of optical nonlinearities in SOAs [4-7]. Much attention has been paid to the nonlinear effect of birefringence induced in SOA [4]. The effective refractive indices for transverse-electric (TE) mode and transverse-magnetic (TM) mode are different form each other due to intrinsic birefringence in SOA and induced birefringence in SOA, thus the polarization changes in SOA for TE and TM modes [4]. This change of nonlinear polarization in the SOA component will result in the appearance of optical logic gate characterized by high speed of response [8-12].

The design of a semiconductor optical amplifier (SOA) component must necessarily pass the modeling phase which allows studying a theoretical characterization of the SOA and anticipating its reactions on the basis of the operating conditions [1]. Mathematical models are required to aid in the design of SOAs and to predict their operational characteristics. The theoretical foundation of SOAs modeling was established in 1980s [1, 13]. Since then, major progress concerning SOA modeling start to focus on the material gain coefficient, spontaneous emission rate and the fraction of spontaneous emissions coupled with the guided

waves in an amplifier. Some numerical simulations which use the Finite Difference Method (FDM) have been studied intensively to solve carrier rate equation and photon traveling wave equations.

In this paper, we propose to make a dynamic characterization of the effect of the nonlinear polarization rotation in SOA by injecting into the component the pump and probe signals of different power and state of polarization at the entering of the SOA. Therefore, this paper is dedicated to the study of the modifications of our static numerical model to take into account the nonlinear effect of birefringence over time in the SOA [4]. Our detailed dynamic numerical model offers a set of equations and an algorithm that predict their behavior. The equations form a theoretical base from which we have coded our model in several files.cpp that the Language C++ executes. The model is used to predict the properties of optical logic gates and will be also beneficial for all other digital components design and optimization.

2. DYNAMIC NUMERICAL MODEL OF SOA
2.1. System equations of SOA.

The polarization is a very important concept when studying the SOA component. This section is dedicated to the study of the modifications to be added to our static model [4] to take into account this polarization effect. The expressions of the coupled mode equations must be modified. For this, we have developed a more detailed model based on the coupled mode equations dependent on both time and polarization. And thus, we can study the nonlinear effect of the induced birefringence and the stability of SOA to use it well as a multifunctional component in optical telecommunications systems. This model treats separately the TE component and TM component of the optical field, introduces different confinement factors for the two polarization states and takes into account the phenomenon of the TE and TM modes energy coupling [4].

The developed model based on the assumption of quasi-stationary, can be seen in Fgure 1.a is summed up in a several section division of the component gain region so as to take into account the non uniform distribution of carrier density and refractive index. This allows describing the propagation of the field of the incident signal through the component until the output interface. The SOA of length L can be decomposed into N_z sections between its two facets.

Figure 1 also represents the configuration to analyze the dynamic characteristics of the short optical pulse amplification of wavelengt λ_1 during its propagation through the SOA with the injection of a continuous wave (CW) of wavelength λ_2 this can be called an assist beam. The assist beam can be injected either in copropagative configuration or in counterpropagative configuration with the pulse of the entering optical signal.
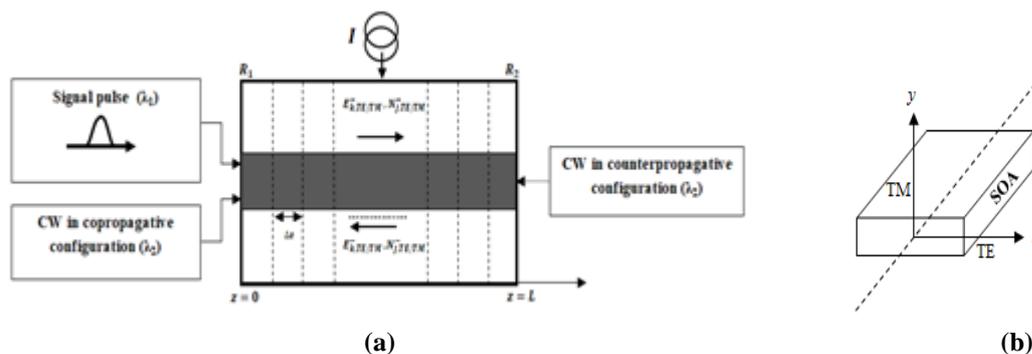
Figure 1. Schema of the optical signals transmission in a SOA (a) and the two polarization directions TE and TM (b)

The pulse of the entering optical signal is a Gaussian pulse of half width FWHM of 10 ps. The field of the entering pulse is given by the following equation [14, 15]:

$$E_{in}(\vartheta, t) = \sqrt{P_0} \times exp\left[-\frac{1}{2}\left(\frac{t}{t_0}\right)^2\right] \times \exp(-j2\pi\vartheta_0 t) \tag{1}$$

With:

- P_0 is the peak input optical power.
- ϑ_0 is the peak frequency.
- t_0 is the duration of the pulse linked with the half width FWHM by the relation: $t_p \cong 1.665 \times t_0$

We thereafter present the mathematical equations that can describe the dynamic behavior of SOA. These differential equations describe the propagation of the optical signal, the amplified spontaneous emission ASE and the evolution of the carrier density and which depend on the time, the space and the two polarization modes (TE mode and TM mode).

To begin with, we decompose the incoming arbitrarily polarized electric field in a TE component and TM component as illustrated in Figure 1.b. These two polarization directions are along the principal axes (*x, y*) that diagonalize the wave propagation in the SOA.

The total electric field is defined by [5]:

$$\vec{E}(\vartheta, z, t) = E_{TE}(\vartheta, z, t)\vec{x} + E_{TM}(\vartheta, z, t)\vec{y} \qquad (2)$$

With: $\begin{cases} E_{TE}(\vartheta, z, t) = E_{in}(\vartheta, t) \times cos(\theta) \times \exp(j\emptyset_x) \\ E_{TM}(\vartheta, z, t) = E_{in}(\vartheta, t) \times sin(\theta) \times \exp(j\emptyset_y) \end{cases}$

Whereas θ is the input polarization angle, $\emptyset_x$ and $\emptyset_y$ are initial phase of input signal for TE mode and TM mode, respectively. In our calculation, in left (input) and right (output) facets of SOA have power reflectivities R_1, and R_2, respectively. The signal wave gets partially transmitted and reflected from the two facets of the amplifier. Due to the input signal, the spatially varying component of the field in the SOA can be decomposed into forward and backward propagating E+, E-, and the traveling-waving equation for TE mode and TM mode are [1, 7] and [14]:

$$\left(\frac{1}{v_g}\frac{d}{dt} \pm \frac{d}{dz}\right)E^{\pm}_{TE/TM}(z, t) = \left\{\left(-j\beta_{TE/TM}(\vartheta, n) + \frac{1}{2}g_{n,TE/TM}(\vartheta, n)\right)E^{\pm}_{TE/TM}(z, t) + \right.$$
$$\left. C_{TM/TE}(\vartheta, n)E^{\pm}_{TM}(z, t)\right\} \qquad (3)$$

Those spontaneous emission photon rates are observed in the following equation:

$$\frac{dN^{\pm}_{j,TE/TM}(z,t)}{dz} = \pm\left\{g_{n,TE/TM}(\vartheta_j, n)N^{\pm}_{j,TE/TM}(z, t) + R_{sp,TE/TM}(\vartheta_j, n)\right\} \qquad (4)$$

Whereas $j = \sqrt{-1}$, C_{TE} and C_{TM} are the coefficients of coupling modes TE-TM and TM-TE respectively [4, 13].

$$C_{TE/TM}(\vartheta, n) = \mp k_r \times exp(\mp j\Delta\beta \times z) \qquad (5)$$

Whereas $\Delta\beta = \beta_{TE}(\vartheta, n) - \beta_{TM}(\vartheta, n)$, k_r is the coupling constant and v_g is the group speed. The other coefficients are defined in [1, 4].

These amplified forward and backward signal waves should meet the following boundary conditions:

$$E^+_{TE/TM}(z = 0, t) = (1 - r_1)E_{in,TE/TM}(t) + r_1 E^-_{TE/TM}(z = 0, t) \qquad (6)$$

$$E^-_{TE/TM}(z = L, t) = r_2 E^+_{TE/TM}(z = L, t) \qquad (7)$$

Similarly, the output signal field to the right of the output facet is:

$$E_{out,TE/TM}(t) = (1 - r_2)E^+_{TE/TM}(z = L, t) \qquad (8)$$

The initial conditions to solve the amplified spontaneous emission noise equations system.
$$N^{\pm}_{TE/TM}(z = 0, t) = R_1 E^{\mp}_{j,TE/TM}(z = 0, t) \qquad (9)$$

The carrier density in section *i* inside the SOA obey the rate equation [1, 4, 12]:

$$\frac{dn(z,t)}{dt} = \frac{I}{edwL} - R(n) - \frac{\Gamma_{TE}}{dw}\left(f_{k,TE}(n) - 2f_{j,TE}(n)\right) - \frac{\Gamma_{TM}}{dw}\left(f_{k,TM}(n) - 2f_{j,TM}(n)\right) \tag{10}$$

Whereas I is the amplifier bias current, d and w are the active region thickness and width, respectively.

The recombination rate term $R(n)$ is given by:

$$R(n) = C_1 \times n + C_2 \times n^2 + C_3 \times n^3 \tag{11}$$

Whereas C_1, C_2 and C_3 are recombination coefficients.
$f_{k,TE}, f_{k,TM}, f_{j,TE}$ and $f_{j,TM}$ are defined by equations [4]:

$$f_{k,TE/TM}(n) = \sum_{k=1}^{N_s} g_{m,TE/TM}(\vartheta_k, n)\left[\left|E_{TE/TM}^+\right|^2 + \left|E_{TE/TM}^-\right|^2\right] \tag{12}$$

$$f_{j,TE/TM}(n) = \sum_{j=0}^{N_m-1} g_{m,TE/TM}(\vartheta_j, n)\left[N_{j,TE/TM}^+ + N_{j,TE/TM}^-\right] \tag{13}$$

With, N_s numbers of signals injected with optical frequencies ϑ ($k = 1$ to N_s) and N_m is an integer that determines the sampling step of the spontaneous emission frequencies. The physical meaning of each of the terms in equation (10) is shown in Table 1.

Table 1. Physical signification of the terms of the carrier density evolution equation.

Terms	Physical meaning
$dn(z,t)/dt$	Variation of carrier density as a function of time and space.
$I/edwL$	Carrier density injected by the bias current.
$R(n)$	Decreasing of carrier density by the spontaneous recombination.
$f_{k,TE/TM}$	Decreased carrier density caused by amplification of signals.
$f_{j,TE/TM}$	Function describing the influence of ASE on carrier density.

The systems of equations (3) and (4) are systems of five partial, nonlinear and coupled equations that do not have an analytic solution. A numerical resolution is then necessary. Partial derivatives appearing in these last equations are approximated by the finite differences in the first order and can be replaced by:

$$\begin{cases} \frac{dE_{TE/TM}^{\pm}(z,t)}{dt} = \pm\frac{E_{TE/TM}^{\pm}(z,t\pm\Delta t) - E_{TE/TM}^{\pm}(z,t)}{\Delta t} \\ \frac{dE_{TE/TM}^{\pm}(z)}{dz} = \pm\frac{E_{TE/TM}^{\pm}(z\pm\Delta z,t) - E_{TE/TM}^{\pm}(z,t)}{\Delta z} \\ \frac{dN_{TE/TM}^{\pm}(z)}{dz} = \pm\frac{N_{TE/TM}^{\pm}(z\pm\Delta z,t) - N_{TE/TM}^{\pm}(z,t)}{\Delta z} \end{cases} \tag{14}$$

Similarly, the evolution equation of carrier density $\frac{dn(z,t)}{dt}$ is approximated by: $\frac{dn(z,t)}{dt} = \frac{n(z,t+\Delta t) - n(z,t)}{\Delta t}$ (15)

2.2. Dynamic of numerical algorithm

In dynamic regime, we estimated the evolution of the carrier density $\frac{dn(z,t)}{dt}$ by the method of FDM (15). The following algorithm, in Figure 2 summarizes the main steps used during the simulation:

Step1: Initialize to transparency, the initial conditions at t = 0.
Step2: Begin iteration of time, then we estimate the signal fields and spontaneous emission photon rates using the method of FDM equations: (16), (17), (18) and (19).
Step3: The results found in the previous step for each iteration of the time are injected into the carrier evolution equation (20), and then the results found are saved for a complete study of the SOA component over time.
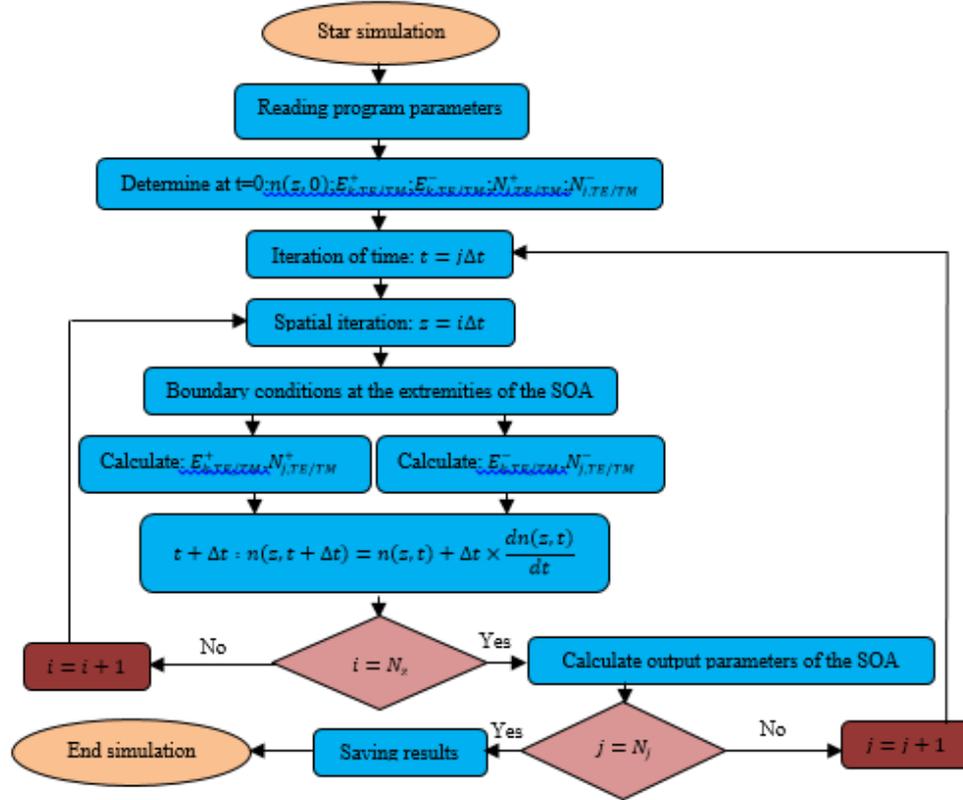
Figure 2. Flowchart of the SOA dynamic model

The SOA geometrical and material parameters used in the model are given in [4], and the time simulation parameters are listed in the Table 2 above.

Table 2. Summary of time simulation parameters

Symbol	Parameter	Value
N_z	Peak input optical power.	80
I	Number of SOA section.	260mA
P_0	Amplifier bias current.	0dBm
n_{in}	Number of iteration of time.	3870
Δt	Not temporal.	0.167ps
$n_{in} \times \Delta t$	Time window.	646ps

3. RESULTS AND DISCUSION

This part will make the subject of the presentation and the interpretation of the results obtained by numerical simulation of our model. The Simulation results showed that the study of dynamic properties of birefringence effects in SOA can help us to overcome many of the inconveniences that reduce the efficiency of the SOA component for its application in modern optical telecommunications systems such as the long recovery time of the gain and the deformation of the outgoing optical pulse. The results show that we can overcome these disadvantages by injecting an assist beam of different power and polarization state.

3.1. Study of the gain recovery time

In this subsection, we will study the gain recovery dynamics of the SOA including the effect of ASE during the passage of a short optical pulse, shown in Figure 3a. The Figure 3b shows the evolution of the fiber-to-fiber gain as a function of time. From this figure, we can notice 3 states of gain: the **state 0** corresponding to a minimum gain which is also called the state of gain compression; **state 1** corresponding to a maximum gain, this is the state of the small-signal gain of the SOA and the last state is that of the passage between the state 0 and the state 1 which corresponds to the gain recovery time.

(a)   **(b)**
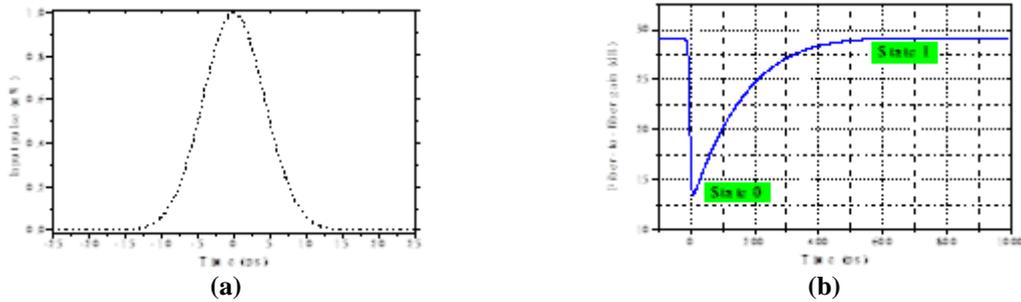
Figure 3. Input optical pulse (**a**) and gain recovery dynamics with the injection of a TE polarized pulse (**b**)

Figure 4 illustrates the longitudinal distribution of carrier density and ASE photon rate at different times of the gain recovery dynamics of figure 3.b. It is noted that after the gain compression, the carrier density and the intensity of the photon rate ASE are weak in left and right facets of the component, which explains a slow gain recovery time but when the intensity of ASE is strong enough in the extremities sections of the SOA, the recombination of the stimulated emission becomes dominant compared to that of spontaneous emission. This makes it possible to accelerate the recovery of the carriers, in particular in the front end where the carrier density goes beyond its state of equilibrium (red curves).

State 0

State 1
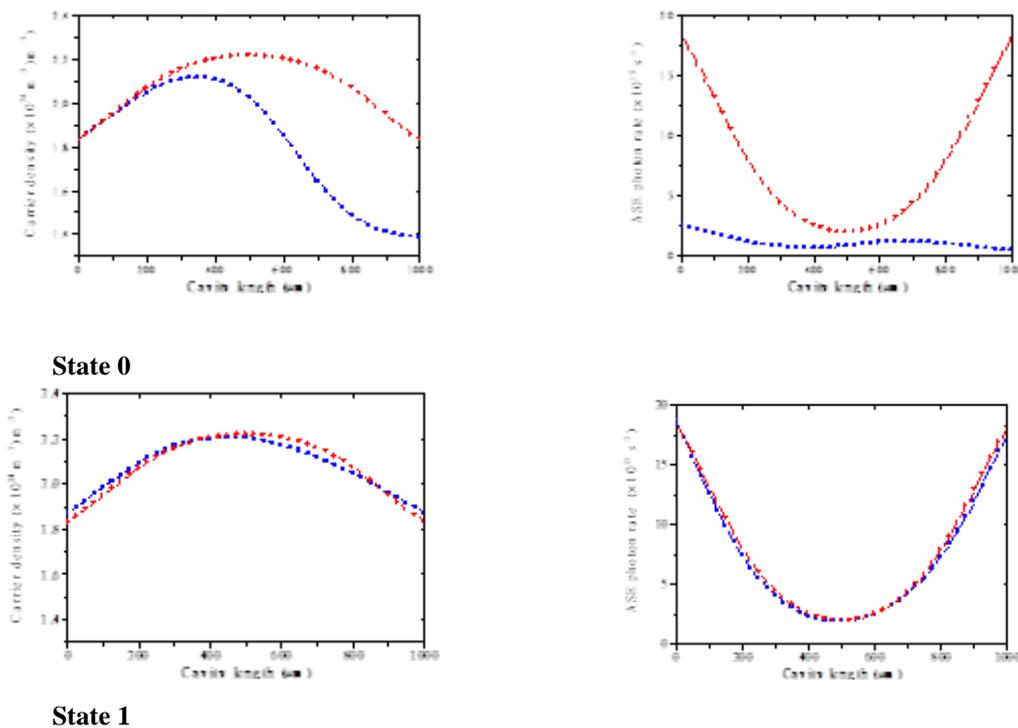
Figure 4. Spatial distribution of carrier density and ASE photon rate for different gain recovery times

Figure 5 shows the gain recovery dynamics with co-propagating or counter-propagating injection of the different continuous power signals. The curves of Figure 5 show that gain recovery time of the SOA is clearly shortened with the increase of the power of assist beam for both configurations. Because, the more power of the assist beam is, the more important the amplification mechanism by stimulated emission. In all cases of figure, this gain recovery time is shorter in counter-propagating configuration. This efficiency is obtained by injecting the power of the assist beam at the output of the SOA, where the pulse signal needs many carriers to avoid gain saturation.

(a): Copropagating configuration   **(b): Counterpropagating configuration**
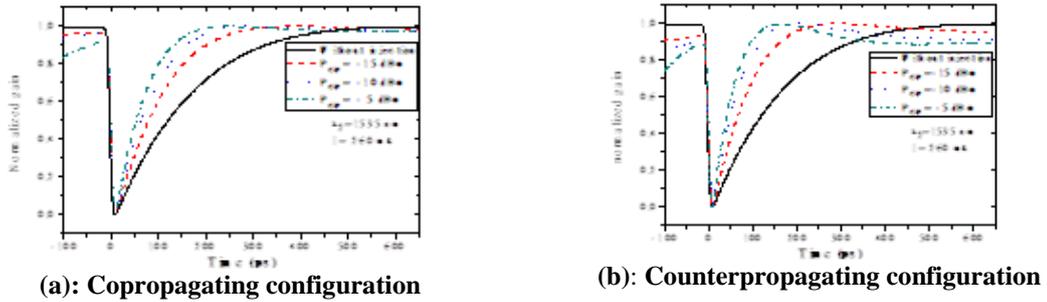
Figure 5. Gain recovery time for different powers of the CW, where the input signals are polarized TE

Subsequently, we will study the effect on the gain recovery time when the input pulse, under different polarization angles of the assist beam.

One can notice for both polarizations of the incoming pulse (TE and TM), that the gain recovery time is remarkably shortened when the assist beam is polarized TE ($\theta cw = 0°$) shown in Figure 6 and the more the polarization angle of the assist beam is, the more important the gain recovery time. Add to this that the counter-propagating injection of the assist beam gives better results for the gain recovery time.

(a): TE polarized pulse   **(b): TM polarized pulse**
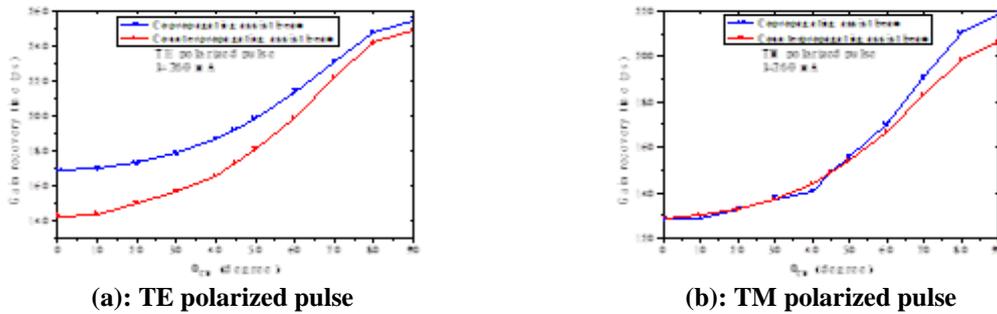
Figure 6. Gain recovery time at different polarizations of CW

3.2. Time characterization of the outgoing optical pulse

In this subsection, we will analyze the temporal characteristics of the short optical pulse amplification in the SOA for different polarizations with and without the injection of a assist beam. We will show further that with the injection of an assist beam in the gain region, we can reduce the deformation of the outgoing optical pulse.

Figure 7 shows the evolution of the output power in the different sections of the SOA for the two polarization cases of the incoming optical pulse without injection of the assist signal. From this figure, it is found that peak power of the outgoing optical pulse becomes more important compared to that of the incoming pulse for the two polarization cases. But we can notice that the injection of the pulse in TE mode presents a great power of the outgoing optical pulse and a remarkable deformation compared to that of the TM mode injection.

(a): TE polarized pulse   **(b): TM polarized pulse**
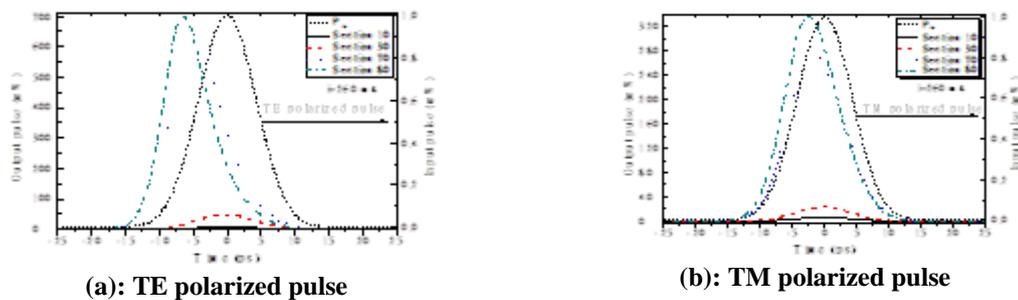
Figure 7. Spatial and temporal distributions of the outgoing optical pulse

Subsequently, we will study the case where the incoming optical pulse is assisted by the injection of an assist beam to reduce the deformation of the outgoing optical pulse of the SOA.

Figure 8 shows the time distribution of the outgoing optical pulse with the injection of the different powers of assist beam in co-propagating and counter-propagating configuration. The curves of this figure show a reduction in the deformation of the outgoing optical pulse and a decrease in peak power as the power of the assist beam is increased. We can notice that the reduction of deformation is clearly remarkable for the counter-propagating configuration. This is due to the decrease of the fast saturation of the carrier density the rising edge of the incoming pulse with the injection of a high power of the assist beam.

| (a): Copropagating configuration | (b): Counterpropagating configuration |
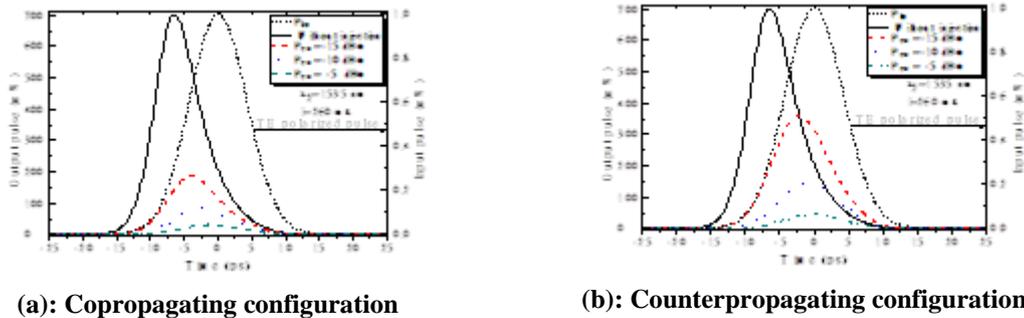
Figure 8. Time distribution of the outgoing optical pulse for different power of CW

Figure 9 illustrates the effect of polarization of an assist beam injected in co-propagating or counter-propagating configuration on the SOA component to which we also injected an optical pulse polarized in a TE. One can notice from figure 9 that the deformation of the outgoing optical pulse is dependent on the polarization of the assist beam. For the two cases of figure. 9, we observe that when the assist beam is polarized TE, the deformation of the outgoing optical pulse is well reduced compared to that polarized TM. This trend comes from the elastic constraints applied to SOA which largely favors TE transitions.

| (a): Copropagating configuration | (b): Counterpropagating configuration |
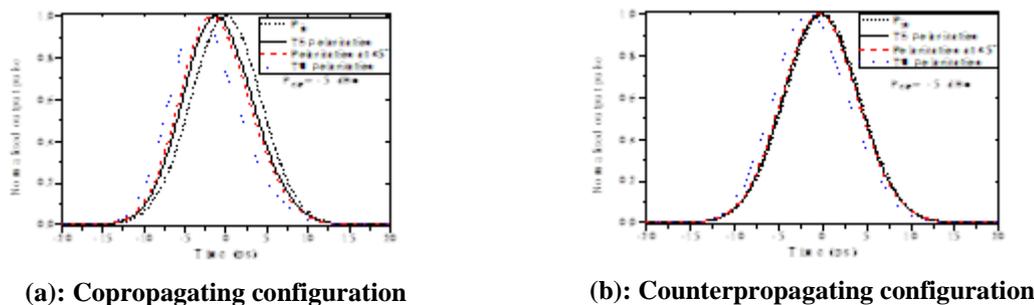
Figure 9. Time distribution of the normalized outgoing optical pulse for different polarization of CW

4. CONCLUSION

After explaining our numerical model in the time domain, we have listed the basic equations necessary to simulate the dynamic behavior of SOA by the FDM method. Subsequently, we have studied the dynamic characterization of the birefringence effects induced in the SOA component to overcome the slow gain recovery time and eventually obtain a deformation as reduced as possible of the outgoing optical pulse. The results of the simulations have shown that we can overcome these drawbacks by the injection of an assist beam in counterpropagation configuration, polarized TE and of a high power.

REFERENCES

[1] A.Elyamani, A. Zatni, "Steady-state of numerical model and the design of a wideband semiconductor optical amplifier using the finite difference method," *Journa of Theoretical and Applied Information technologie*, vol. 51, pp. 400-409, 2013.

[2] Agrawal, G.P, *Fiber-Optic Communication Systems, Volume 1. 3rd Edn*, WileyInterscience, New York, USA, 2002.

[3] Ronald W. Waynant (Author), Marwood N. Ediger (Editor), Ronald Waynant (Author), *Electro-optics Handbook, Optical and ElectroOptical Engineering Series, 1st edition*, 1994.

[4] A.Elyamani and A.Zatni, "Static characterization of the birefringence effect in the Semiconductor Optical Amplifier Using the Finite Difference Method," *International Journalof Electrical and Computer Engineering, Scopus*, vol. 5, no. 1, pp. 38-45, Feb 2015.

[5] H. Lirong and H. Dexiu, "Spectral broadening of ultrashort optical pulse due to birefringence in semiconductor optical amplifiers," *optics communications*, vol. 223, pp. 295-300, 2003.

[6] L.Q. Guo and M.J. Connelly, "A Mueller-Matrix Formalism for modeling Polarization Azimuth and Ellipticity Angle in Semiconductor Optical Amplifiers in Pump-Probe Scheme," *Journal of Lightwave Technology*, vol. 25, pp. 410-420, 2007.

[7] Deng, Ye, Li, Ming, and ShuqianSun, "Fully characterization of a DFB-SOA based active optical filter," *IEEE Opto-Electronics and Communications*, pp. 1−3, 2015.

[8] Ankur Saharia and Ritu Sharma, "An Approach for the Realisation of NAND,NOR & AND Gate Using Semicponductor Optical Amplifier & Band Pass Filter," *2014 Sixth International Conference on Computational Intelligence and Communication Networks,* 2014.

[9] Saumya Saxena, "All Optical EX-OR Gate based on Four Wave Mixing Non Linear Effect in Semiconductor Optical Amplifier (SOA)," *IEEE International Conference on Power, Control, Signals and Instrumentation Engineering,* ICPCSI-2017.

[10] M. A. Esmail, A. Ragheb, and H. Fathallah, "Demonstration of Photonics-Based Switching of 5G Signal over Hybrid All-Optical Network," *IEEE Photonics Technology Letters*, 2018.

[11] Dhoumendra Mandal, Sumana Mandal, and Sisir Kumar Garai, "Design of all-optical one bit binary comparator using reversible logic gates," 1st International Conference on Electronics, Materials Engineering and Nano-Technology (IEMENTech), 2017.

[12] S. Pitris, C. Vagionas, Student Member , IEEE, "WDM-enabled Optical RAM at 5 Gb/s Using a Monolithic InP Flip-Flop Chip", 1943-0655 (c) 2015 IEEE.

[13] Dong-Xue Wang, JOHN A.Buck, Kevin Brennan, and Ian Ferguson, "A numerical model of wavelength converters based on cross-gain modulation in semiconductor optical amplifiers," *Applied Optics Engineer*, vol. 45, pp.47014-4708, 2006.

[14] F. Ginovart, J.C. Simon, and I. Valiente, "Gain recovery dynamics in semiconductor optical amplifier," *optics communications*, vol. 199, pp. 111-115, 2001.

[15] Hui Wang, Jian Wu, and Jintong Lin, "Spectral Characteristics of Optical Pulse Amplification in SOA Under Assist Light Injection," *JOURNAL OF LIGHTWAVE TECHNOLOGY,* vol. 23, no. 9, Sep 2005.

BIOGRAPHIES OF AUTHORS

Abdenbi ELYAMANI was born in Kenitra, Morocco, on January 1st, 1984. He received a PhD in electronics and telecommunication at the faculty of sciences University Ibnou Zohr in 2016. He has been teaching physics chemistry at high school for 8 years. His research interests include design, characterization, modelling and optimization of optoelectronic components and fibre optic communications systems.

Abdelkarim ZATNI was educated at the Telecom Bretagne University France. He obtained a PhD at the National School of Engineers of Brest France in 1994. He has been teaching for 24 years at the faculty of sciences University Ibnou Zohr. He conducts his research and teaches computer science and telecommunication.